``

# Two-Dimensional β-PdX$_2$ (X = S, Te) Monolayers for Efficient Solar Energy Conversion Applications

Mukesh Jakhar and Ashok Kumar[*]

*Department of Physics, School of Basic Sciences, Central University of Punjab, Bathinda, 151401, India*

(February 24, 2022)

*Corresponding Author:

ashokphy@cup.edu.in (Ashok Kumar)

# Structure and Stability

**Table S1.** Structural properties of β-PdX$_2$ bulk and monolayer.

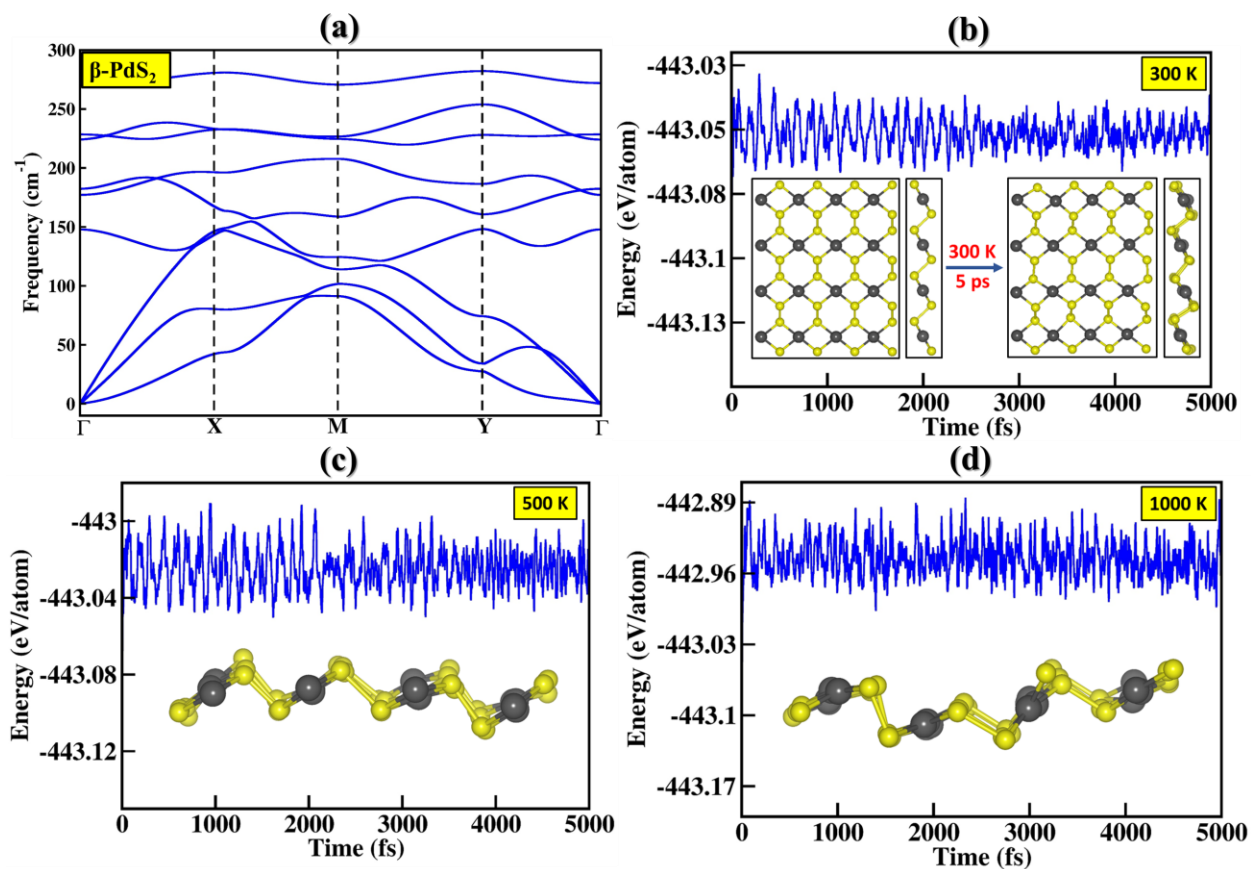| Structures | Lattice Constants (Bulk) | | | Lattice Constants (Monolayer) | | Pd-X, X-X (X=S,Te) (Bulk) | Pd-X, X-X (X=S,Te) (Monolayer) |
|---|---|---|---|---|---|---|---|
| | a (Å) | b (Å) | c (Å) | a (Å) | b (Å) | | |
| **β-PdS$_2$** | 3.49 | 4.32 | 5.0 | 3.48 | 4.31 | 2.35, 2.11 | 2.35, 2.11 |
| **β-PdTe$_2$** | 3.96 | 4.93 | 5.42 | 3.95 | 4.86 | 2.64, 2.86 | 2.64, 2.80 |



**Fig. S1** (a) The calculated phonon dispersion spectra of β-PdS$_2$ monolayer. The AIMD total energy fluctuations at (b) 300 K, (c) 500 K, and (d) 1000 K with the snapshot of β-PdS$_2$ monolayer before and after a 5000 fs AIMD simulations.
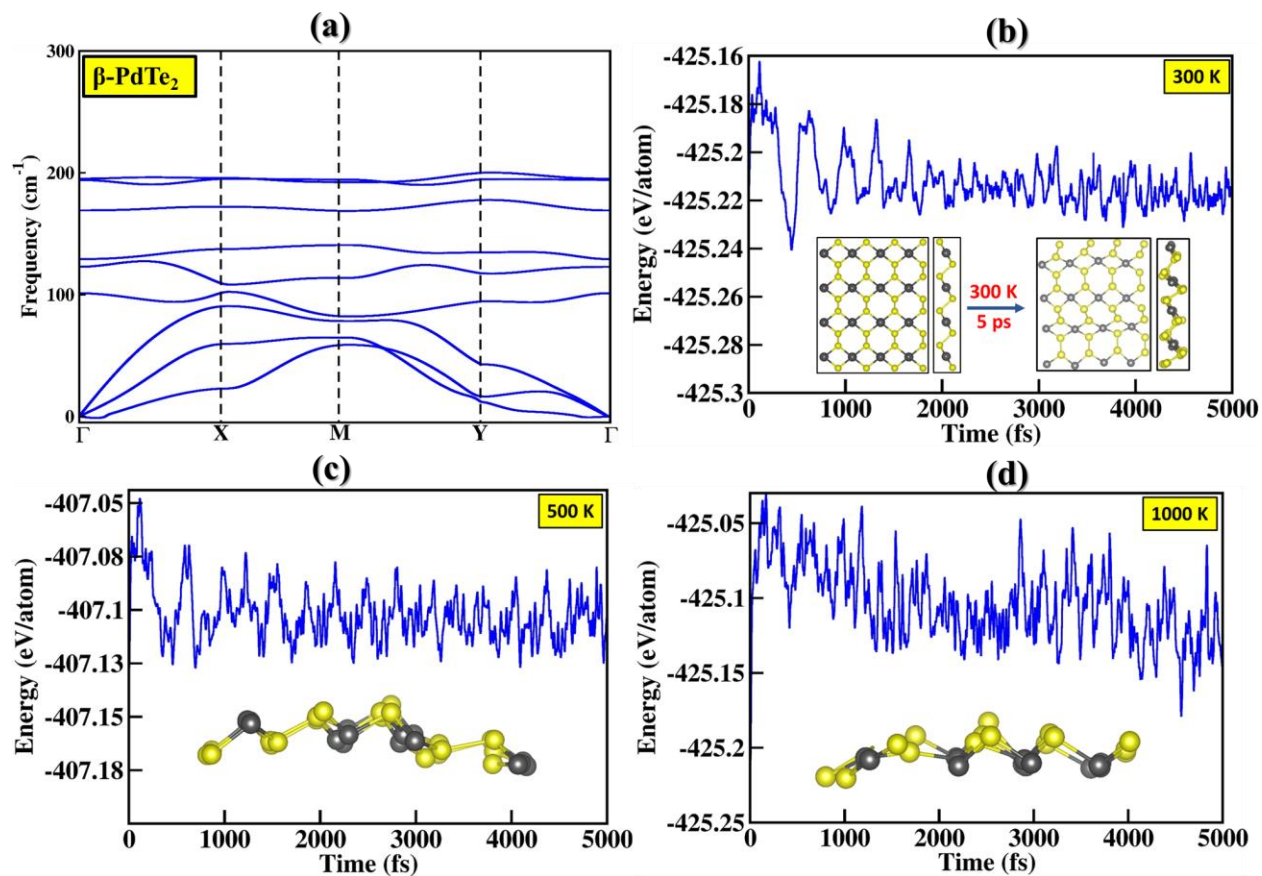
**Fig. S2** (a) The calculated phonon dispersion spectra of β-PdTe$_2$ monolayer. The AIMD kinetic and total energy fluctuations at (b) 300 K, (c) 500 K, and (d) 1000 K with the snapshot of β-PdTe$_2$ monolayer before and after a 5000 fs AIMD simulations.

## Electronic Structure with SOC



**Fig. S3** The calculated band structure for β-PdS$_2$ monolayer with spin-orbital coupling (SOC) (red) and without SOC (black) extracted from PBE functional.
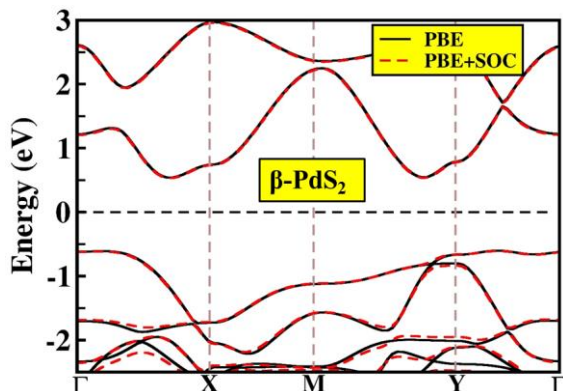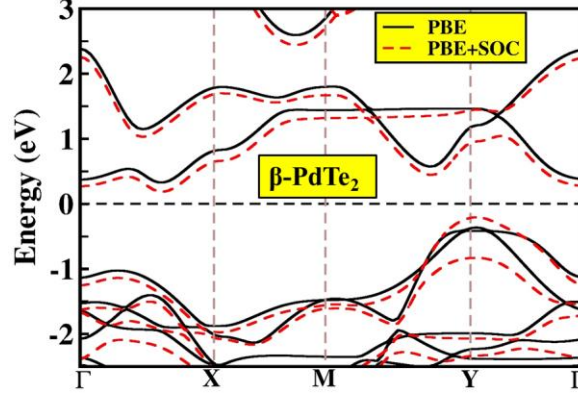
``



**Fig. S4** The calculated band structure for β-PdTe₂ monolayer with spin-orbital coupling (SOC) (red) and without SOC (black) extracted from PBE functional.

## Carrier Mobilities

The charge carrier mobilities have been calculated using $\mu_{2D} = \frac{e\hbar^3 C_{2D}}{K_B T m^* m_a^* E_i^2}$ where, $C_{2D}$ is the elastic modulus of the material along transport direction and is given by $C_{2D} = \frac{1}{S_0}(\frac{\delta^2 E_{total}}{\delta\epsilon^2})$. $E_{total}$, $\epsilon$, and $S_0$ are the total energy, uniaxial strain, and the unstrained unit cell area, respectively. $E_i$ is the deformation potential which is defined as $E_i \frac{\delta E_{edge}}{\delta\epsilon}$, where $E_{edge}$ is the energy of VBM or CBM. $m^*$ is the effective mass in the transport direction (i.e., either along x or y direction), and $m_a^*$ is the average effective mass given by $\sqrt{m_x^* m_y^*}$ .

**Table S2:** β-PdX₂ monolayer: The effective mass ($m^*$), the elastic modulus of the material ($C_{2D}$), the deformation potential ($E_i$ ), and the charge carrier mobilities ($\mu_{2D}$).

| Material | Charge Type | $m^*/m_0$ | $C_{2D}$ (J/m²) | $E_i$ (eV) | $\mu_{2D}(cm^2V^{-1}S^{-1})$ |
|---|---|---|---|---|---|
| β -PdS₂ | h(x) | 5.25 | 46.14 | 1.565 | 25.75 |
| | e(x) | 0.46 | 46.14 | 2.55 | 1041.87 |
| | h(y) | 1.72 | 26.56 | 2.0 | 27.60 |
| | e(y) | 0.22 | 26.56 | 2.7 | 1069.15 |
| β -PdTe₂ | h(x) | 0.84 | 40.55 | 4.34 | 107.92 |
| | e(x) | 0.27 | 40.55 | 2.0 | 1258.47 |
| | h(y) | 0.32 | 8.89 | 1.48 | 544.86 |
| | e(y) | 1.56 | 8.89 | 3.38 | 16.71 |

## Thermodynamic Oxidation and Reduction Potentials of β-PdS₂ monolayer in Aqueous Solution
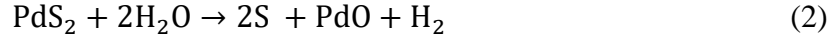
In the light of componential analysis and the modified method mentioned in the previous literature[1], we assume the β-PdS₂ monolayer can be oxidized and reduced by the photogenerated holes and electrons through the following reactions:
Reduction

$$PdS_2 + 2H_2 \rightarrow Pd + 2\,(H_2S) \tag{1}$$

Oxidation

$$PdS_2 + 2H_2O \rightarrow 2S + PdO + H_2 \tag{2}$$

The thermodynamic reduction potential of the β-PdS$_2$ monolayer reduction potential ($\phi^{re}$) and oxidation potential ($\phi^{ox}$) could be calculated as follows

$$\phi^{re} = -[\Delta_f G^0(Pd) + 2\Delta_f G^0(H_2S) - \Delta_f G^0(PdS_2) - 2\Delta_f G^0(H_2)]/4eF + \phi(H^+/H_2) \tag{3}$$

$$\phi^{ox} = [2\Delta_f G^0(S) + \Delta_f G^0(PdO) + \Delta_f G^0(H_2) - \Delta_f G^0(PdS_2) - 2\Delta_f G^0(H_2O)]/4eF + \phi(H^+/H_2) \tag{..(4)}$$

where $\Delta_f G^0(Pd)$, $\Delta_f G^0(H_2S)$, $\Delta_f G^0(PdS_2)$, $\Delta_f G^0(S)$, $\Delta_f G^0(PdO)$ and $\Delta_f G^0(H_2)$ mean the standard molar Gibbs energy of formation of Pd, H$_2$S, PdS$_2$, S, PdO, $\Delta_f G^0(H_2O)$, and H$_2$. As listed in Table S3, the $\Delta_f G^0(Pd)$, $\Delta_f G^0(H_2S)$, $\Delta_f G^0(S)$, $\Delta_f G^0(PdO)$ and $\Delta_f G^0(H_2)$ could be found in the handbook[2]. The standard molar Gibbs energy of formation of β-PdS$_2$ monolayer is approximated by its formation energy ($E_f$), which is defined as follows:

$$E_f = E_{PdS_2} - E_{Pd} - 2E_S/3 \tag{5}$$

where $E_{PdS_2}$ means the total energy of β-PdS$_2$ unit cell, while $E_{Pd}$, and $E_S$ separately stand for the energy of Pd, and S in their stable phases. $E_{Pd}$, and $E_S$ are -3442.444, and -274.251 eV/atom, respectively. The total energy of β-PdS$_2$ unit cell ($E_{PdS_2}$) is -4002.969 eV/unit. Therefore, the formation energy of β-PdS$_2$ monolayer ($E_f$) is -4.0 eV/aotm. ($H^+/H_2$) is 0 V relative to the normal hydrogen electrode (NHE) potential. F and e represent the Faraday constant and the elemental charge, respectively. After plugging the relevant values into Equation 3-4, $\phi^{re}$, $\phi^{ox}$ is obtained as -1.707 V and 3.07 V (relative to NHE). The $\phi^{re}$ is smaller than 0 V, while the $\phi^{ox}$ is larger than 1.23 V, indicating the strong resistance to photoinduced corrosion of β-PdS$_2$ monolayer.

**Table S3** Standard Molar Gibbs Energy of Formation ($\Delta_f G^0$) at 298.15 K in kJ/mol.

| Molecular Formula | $\Delta_f G^0$ | Molecular Formula | $\Delta_f G^0$ |
|---|---|---|---|
| Pd | 339.7 | H$_2$O | -237.1 |
| H$_2$S | -33.4 | S | 236.7 |
| H$_2$ | 0 | PdO | 325.9 |

## Adsorption/Intercalation Energies

**Table S4**. Binding energies of adsorption, intercalation and adspt+intclt models for (001) surface of β-PdS$_2$.

| H$_2$O Molecules | Binding Energy per H$_2$O Molecules (eV) | | |
|---|---|---|---|
| | Adsorption | Intercalation | Adspt+Intclt |
| 1 | -0.059 | -0.047 | - |
| 2 | -0.34 | -0.35 | - |
| 3 | -0.82 | -0.81 | - |
| 4 | -1.40 | -1.43 | - |
| 8 | - | - | -2.82 |

# Gibbs Free energy Calculations

To further clarify the thermodynamics of water redox reactions on the $\beta$-PdS$_2$, we calculate the Gibbs free energy change of HER and OER at pH 0 to 7, with and without the effect of light irradiation. The hydrogen electrode model developed by Nørskov et al. is adopted to calculate the Gibbs free energy, as follows:
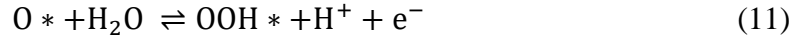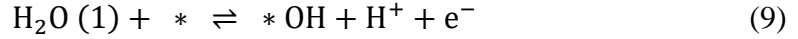
$$\Delta G = \Delta E + \Delta E_{ZPE} - T\Delta S + \Delta G_U + \Delta G_{pH} \tag{6}$$

where $\Delta E$ represents the DFT computed total energy difference, and $\Delta E_{ZPE}$ and $T\Delta S$ are the zero-point energy difference and the entropy, respectively $\Delta G_U$ ($\Delta G_U = -eU$) denotes the extra potential bias provided by an electron in the electrode, where U is the electrode potential relative to the standard hydrogen electrode (SHE). $\Delta G_{pH}$ represents the contribution of Gibbs free energy at different pH concentrations.

The HER half-reaction can be decomposed into a two-electron step, and the reaction equation can be written as:

$$H^+ + e^- + \ * \ \leftrightharpoons \ *H \tag{7}$$
$$*H + H^+ + e^- \rightleftharpoons H_2 \tag{8}$$

The OER half-reaction can be decomposed into a four-electron step, and the reaction equation can be written as:

$$H_2O \ (1) + \ * \ \rightleftharpoons \ *OH + H^+ + e^- \tag{9}$$
$$*OH \rightleftharpoons \ *O + H^+ + e^- \tag{10}$$
$$O* + H_2O \rightleftharpoons OOH* + H^+ + e^- \tag{11}$$
$$*OOH \rightleftharpoons \ * + O_2(g) + e^- \tag{12}$$

Gibbs free energy changes $\Delta G$ for each intermediate and each step in the OER process were calculated using the following equations

$$\Delta G_{OH} = G(*OH) + G(H^+ + e^-) - G(*) - G(H_2O)$$
$$\Delta G_O = G(*O) + 2G(H^+ + e^-) - G(*) - G(H_2O)$$
$$\Delta G_{OOH} = G(*OOH) + 3G(H^+ + e^-) - G(*) - 2G(H_2O)$$

Then, considering the effect of electrode potential (U) and pH, the free energy change for OER electrochemical steps can be expressed as:

$$\Delta G_1 = \Delta G_{OH} = \Delta G_{OH} = G(*OH) + G(H^+ + e^-) - G(*) - G(H_2O) - \Delta G_U - \Delta G_{pH}$$
$$\Delta G_2 = \Delta G_O - \Delta G_{OH} = G(*O) + G(H^+ + e^-) - G(*OH) - \Delta G_U - \Delta G_{pH}$$
$$\Delta G_3 = \Delta G_{OOH} - \Delta G_O = G(*OOH) + G(H^+ + e^-) - G(*O) - G(H_2O) - \Delta G_U - \Delta G_{pH}$$
$$\Delta G_4 = 4.92 \ [eV] + [G(*) + 2G(H_2O)] - [G(*OOH) + 3G(H^+ + e^-)] - [\Delta G_U + \Delta G_{pH}]$$

``

**Table S5**. Zero-pint energy correction ($E_{ZPE}$), entropy contribution (TS, T=298.15K), total energy (E), and the Gibbs free energy (G) of molecules and adsorbents on β -PdS$_2$ monolayer.

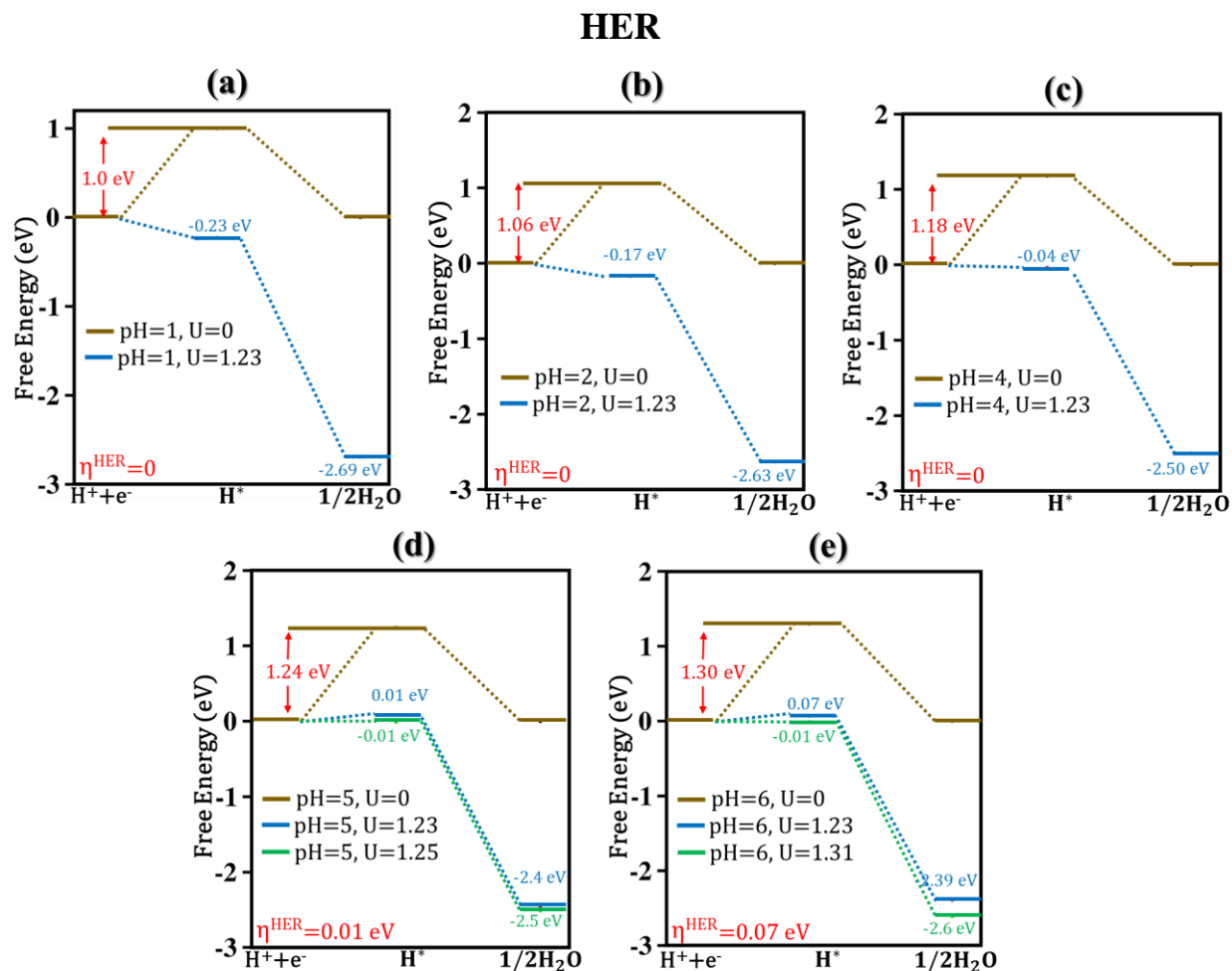| Adsorbents | $E_{ZPE}$ (eV) | −TS (eV) | E (eV) | G (eV) |
|---|---|---|---|---|
| H$_2$ | 0.31 | -0.41 | -31.7593720 | -31.8593720 |
| H$_2$O | 0.62 | -0.67 | -467.3122953 | -467.362295 |
| * | - | - | -16018.508215 | -16018.508215 |
| *O | 0.09 | -0.00 | -16452.228387 | -16452.138387 |
| *OH | 0.36 | -0.00 | -16468.11140343 | -16467.751403 |
| *OOH | 0.46 | -0.21 | -16900.195346 | -16899.945346 |
| *H | 0.23 | -0.00 | -16033.713824 | -16033.483824 |

## HER



**Fig. S5** Free energy profile on β-PdS$_2$ monolayer for HER at (a) pH=1 (b) pH = 2 (c) pH=4 (d) pH=5 (e) pH=6.
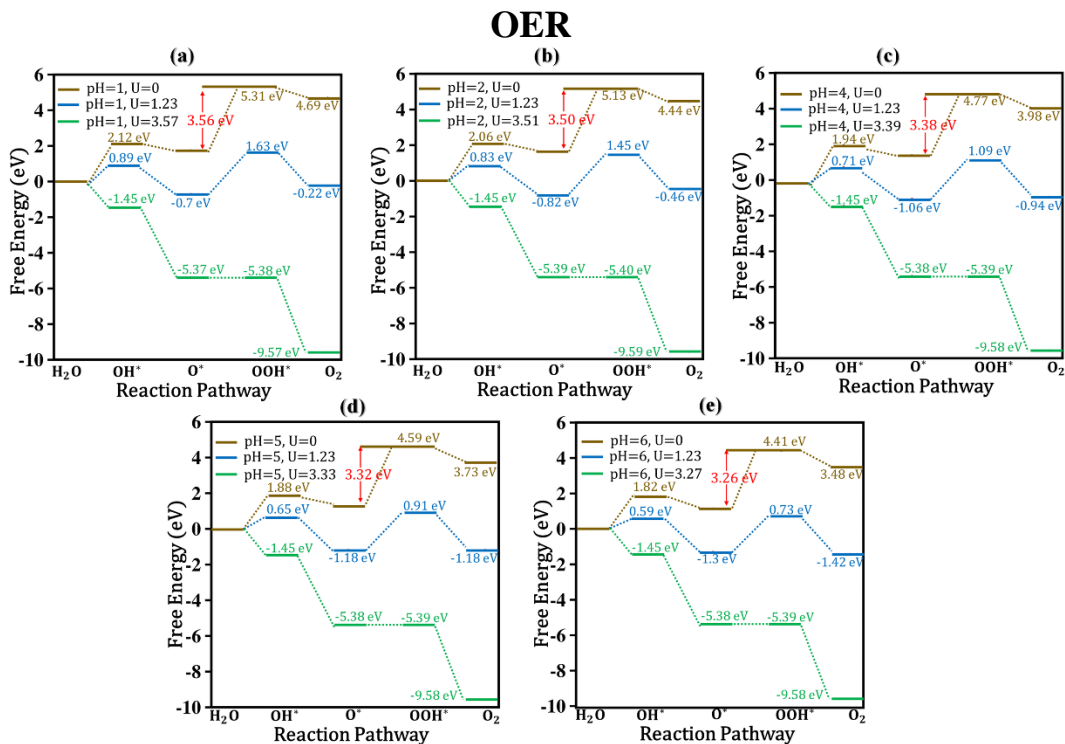
7

# OER



**Fig. S6** Free energy profile on β-PdS$_2$ monolayer for OER at (a) pH=1 (b) pH = 2 (c) pH=4 (d) pH=5 (e) pH=6.

# Solar to Hydrogen Efficiency

**Table S6.** Calculated the Over-Potential for HER $\chi(H_2)$ and OER $\chi(O_2)$, $E$ is the energy of photons of β-PdS$_2$ monolayer with the function of pH. The energy conversion efficiency of light absorption ($\eta_{abs}$), carrier utilization ($\eta_{cu}$), and STH ($\eta_{STH}$).

| pH | $\chi(H_2)$ (eV) | $\chi(O_2)$ (eV) | $E$ (eV) | $\eta_{abs}$ (%) | $\eta_{cu}$ (%) | $\eta_{STH}$ (%) |
|---|---|---|---|---|---|---|
| 0 | 0.45 | 0.42 | 2.28 | 32.35 | 35.28 | 11.41 |
| 1 | 0.39 | 0.48 | 2.22 | 32.35 | 39.17 | 12.67 |
| 2 | 0.33 | 0.54 | 2.16 | 32.35 | 43.08 | 13.93 |
| 3 | 0.27 | 0.6 | 2.10 | 32.35 | 47.58 | 15.39 |
| 4 | 0.21 | 0.65 | 2.10 | 32.35 | 47.58 | 15.39 |
| 5 | 0.16 | 0.715 | 2.14 | 32.35 | 44.39 | 14.36 |
| 6 | 0.098 | 0.774 | 2.20 | 32.35 | 40.47 | 13.09 |
| 7 | 0.039 | 0.833 | 2.26 | 32.35 | 36.57 | 11.83 |

The STH efficiency is considered under the situation of 100% efficiency of the catalytic reaction.[2, 3] $\eta_{STH}$ is estimated by $\eta_{STH} = \eta_{abs} \times \eta_{cu}$ where $\eta_{abs}$ is the efficiency of light absorption and $\eta_{cu}$ is carrier utilization. The efficiency of light absorption ($\eta_{abs}$) is defined as

$$\eta_{abs} = \frac{\int_{E_g}^{\infty} P(\hbar\omega)d(\hbar\omega)}{\int_0^{\infty} P(\hbar\omega)d(\hbar\omega)}$$

where $P(\hbar\omega)$ is the AM1.5G solar energy flux at the photon energy $\hbar\omega$ and $E_g$ is the band gap of semiconductors.

The efficiency of carrier utilization as $(\eta_{cu})$ is defined as

$$\eta_{cu} = \frac{\Delta G \int_{E}^{\infty} \frac{P(\hbar\omega)}{\hbar\omega} d(\hbar\omega)}{\int_{E_g}^{\infty} P(\hbar\omega)d(\hbar\omega)}$$

Where $\Delta G$ is the potential difference for water splitting (1.23 eV) and $E$ is the energy of photons used for water splitting. $E$ is determined by

$$E = \begin{cases} E_g, (\chi(H_2) \geq 0.2, \chi(O_2) \geq 0.6) \\ E_g + 0.2 - c, (\chi(H_2) < 0.2, \chi(O_2) \geq 0.6) \\ E_g + 0.6 - \chi(O_2), (\chi(H_2) \geq 0.2, \chi(O_2) < 0.6) \\ E_g + 0.8 - \chi(H_2) - \chi(O_2), (\chi(H_2) < 0.2, \chi(O_2) < 0.6) \end{cases}$$

where $\chi(H_2)$ is overpotential for HER, and $\chi(O_2)$ is overpotential for oxygen evolution reaction (OER). Considering the previous experiments and theoretical calculations reports, the required overpotentials for HER and OER are assumed to be 0.2 and 0.6 eV, respectively[4, 5].
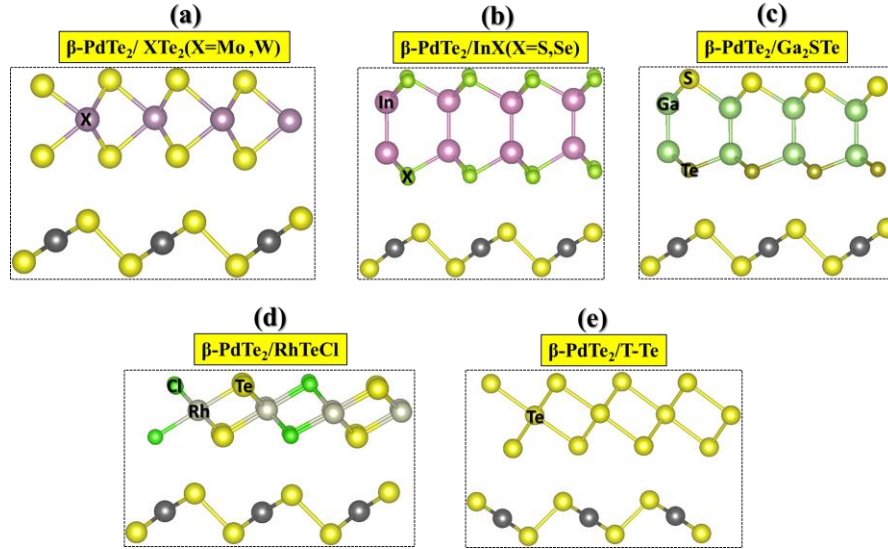
## Excitonic Solar Cell



**Fig. S7** Atomic configurations of (a) β-PdTe$_2$/XTe$_2$ (X=Mo,W) (b) β-PdTe$_2$/InX (X=S,Se) (c) β-PdTe$_2$/Ga$_2$STe (d) β-PdTe$_2$/RhTeCl and (e) β-PdTe$_2$/T-Te heterostructures.
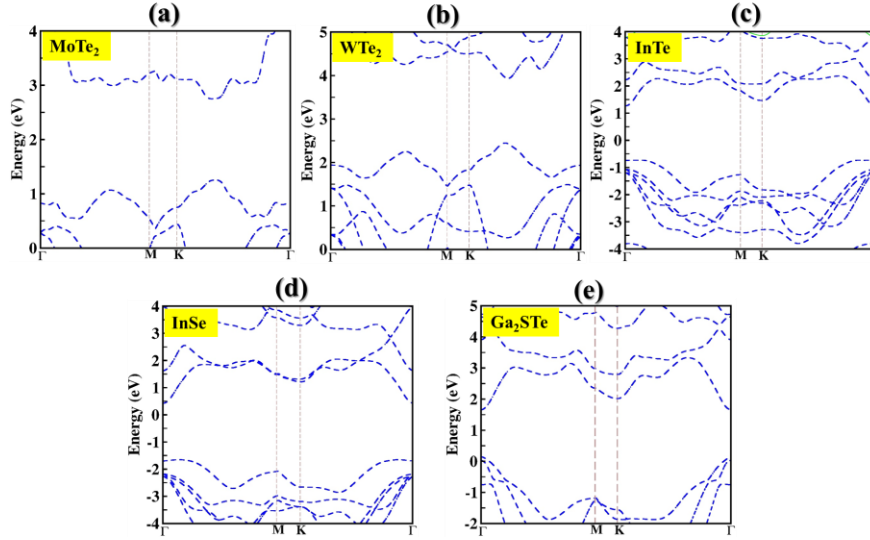
**Fig. S8** The calculated band structure of monolayer (a) $MoTe_2$ (b) $WTe_2$ (c) InTe (d) InSe (e) $Ga_2STe$ using HSE06 functional.

**Table S7:** Calculated lattice parameters, and bandgap ($E_g$) values for optimized TMDs monolayers and lattice mismatch, interlayer distance (d) and binding energy $E_b$ of β-$PdTe_2$ with TMDs heterostructure.

| TMDs | Lattice Parameters | | $E_g(eV)$ | CBM | VBM | Lattice Mismatch (%) | $d(\text{Å})$ | $E_b$ (meV/ atom) |
|---|---|---|---|---|---|---|---|---|
| | $a(\text{Å})$ | $b(\text{Å})$ | | | | | | |
| $MoTe_2$ | 3.55 (3.54)[6] | 6.16 (6.14)[6] | 1.51 (1.50)[6] | -3.86 | -5.37 | 5.44 | 2.73 | 330 |
| $WTe_2$ | 3.56 (3.55)[6] | 6.16 (6.15)[6] | 1.49 (1.47)[6] | -3.75 | -5.24 | 5.58 | 2.71 | 370 |
| $Ga_2STe$ | 3.85 (3.89)[7] | 6.72 | 1.51 (1.61)[7] | -4.25 (-4.29)[7] | -5.76 (-5.90)[7] | 2.25 | 3.01 | 58 |
| InSe | 4.08 (4.08)[7] | 7.07 | 2.10 (2.19)[7] | -4.37 (-4.27)[7] | -6.55 (-6.46)[7] | 3.88 | 3.14 | 9 |
| InTe | 4.38 (4.38)[7] | 7.58 | 2.00 (2.01)[7] | -4.05 | -6.05 | 4.89 | 2.97 | 20 |
| RhTeCl | 3.70 (3.67)[8] | 6.72 (6.65)[8] | 2.23 (2.49)[8] | -4.27 (-4.01)[8] | -6.50 (-6.50)[8] | 4.15 | 2.76 | 60 |
| T-Te | 4.25 (4.23)[9] | 7.36 | 1.01 (1.11)[9] | -4.26 | -5.27 | 3.96 | 2.89 | 9 |
| β-$PdS_2$ | 3.49 | 4.32 | 2.10 | -3.98 | -6.09 | 12.0 | 2.60 | 53 |

``

**Table S8.** The conduction band offsets ($\Delta E_c$), and percentage PCEs of the heterostructure of the monolayer of $\beta$-PdTe$_2$ with different TMDs

| System | $\Delta E_c$ (eV) | PCE% |
|---|---|---|
| $\beta$-PdTe$_2$/ MoTe$_2$ | 0.11 | 20.59 |
| $\beta$-PdTe$_2$/ WTe$_2$ | 0.001 | 23.14 |
| $\beta$-PdTe$_2$/Ga$_2$STe | 0.50 | 11.47 |
| $\beta$-PdTe$_2$/InSe | 0.63 | 8.42 |
| $\beta$-PdTe$_2$/InTe | 0.31 | 15.92 |
| $\beta$-PdTe$_2$/RhTeCl | 0.52 | 10.99 |
| $\beta$-PdTe$_2$/T-Te | 0.52 | 10.99 |
| $\beta$-PdTe$_2$/ $\beta$-PdS$_2$ | 0.23 | 17.79 |

**References**

1. S. Chen and L.-W. Wang, *Chemistry of Materials*, 2012, **24**, 3659-3666.
2. Z. Chen, T. F. Jaramillo, T. G. Deutsch, A. Kleiman-Shwarsctein, A. J. Forman, N. Gaillard, R. Garland, K. Takanabe, C. Heske and M. Sunkara, *Journal of Materials Research*, 2010, **25**, 3.
3. C.-F. Fu, J. Sun, Q. Luo, X. Li, W. Hu and J. Yang, *Nano letters*, 2018, **18**, 6312-6317.
4. C. C. McCrory, S. Jung, J. C. Peters and T. F. Jaramillo, *Journal of the American Chemical Society*, 2013, **135**, 16977-16987.
5. Y. Zheng, Y. Jiao, M. Jaroniec and S. Z. Qiao, *Angewandte Chemie International Edition*, 2015, **54**, 52-65.
6. H. Huang, X. Fan, D. J. Singh, H. Chen, Q. Jiang and W. Zheng, *Physical Chemistry Chemical Physics*, 2016, **18**, 4086-4094.
7. A. Huang, W. Shi and Z. Wang, *The Journal of Physical Chemistry C*, 2019, **123**, 11388-11396.
8. H. Yang, Y. Ma, Y. Liang, B. Huang and Y. Dai, *ACS applied materials & interfaces*, 2019, **11**, 37901-37907.
9. J. Singh, P. Jamdagni, M. Jakhar and A. Kumar, *Physical Chemistry Chemical Physics*, 2020, **22**, 5749-5755.